DOI: 10.1364/JOSAB.32.002488

Journal of the Optical Society of America B
OPTICAL PHYSICS

Reflectionless quasiconformal carpet cloak via parameterization strategy

MATEUS A. F. C. JUNQUEIRA,[1] LUCAS H. GABRIELLI,[2] AND DANILO H. SPADOTI[1,*]

[1]Institute of Systems Engineering and Information Technology, Federal University of Itajubá, Itajubá, MG, Brazil
[2]School of Electrical and Computer Engineering, University of Campinas, Campinas, SP, Brazil
*Corresponding author: spadoti@unifei.edu.br

Received 10 August 2015; revised 15 October 2015; accepted 17 October 2015; posted 21 October 2015 (Doc. ID 247639); published 18 November 2015

In this work the possibility of using both the parameterization function and the least squares method to achieve a quasiconformal carpet cloak via a transformation optical design is demonstrated. The parameterization strategy allows us to obtain a continuous interface around the media, and, therefore, the resulting structure is reflectionless. Polynomial series are added to the coordinate transformation functions, providing a number of degrees of freedom (DoF) without modifying the device boundary conditions. The anisotropy reduction effects over the coordinate transformation are analyzed for different numbers of DoF in the parameterization function. The method's connection with the Riemann mapping theorem is also studied. Our results indicate that anisotropy can be reduced to very close to zero with increasing DoF without incurring edge reflections around the carpet cloak.

OCIS codes: (230.3205) Invisibility cloaks; (230.0230) Optical devices; (000.3860) Mathematical methods in physics; (160.3918) Metamaterials; (160.1190) Anisotropic optical materials.

http://dx.doi.org/10.1364/JOSAB.32.002488

1. INTRODUCTION

Transformation optics (TO) [1,2] is a technique to design optical devices and to control electromagnetic fields using coordinate transformations. The theory is based on the fact that Maxwell's equations are invariant under coordinate transformations, and it is concisely described by differential geometry. It is possible to interpret the parameters of the transformation geometry, such as the metric tensor, as a remapping into material properties for the resulting medium, where the electromagnetic fields will propagate as if in the distorted space. TO allows exotic theoretic applications, such as the well-known cloaking [3–7], and perfect lenses [8,9]. Other TO applications are optical waveguide devices [10–14], lenses [15,16], and splitters [17,18].

TO often results in media with uncommon material requirements, among which are electric and magnetic properties with dependence on position and direction, i.e., inhomogeneous anisotropic magnetic materials, and materials with negative indexes of refraction [1,2]. The use of metamaterials, which are artificial materials with controlled properties, is a possible approach to meet those requirements [19,20]. However, current fabrication technologies are still limited in resolution and number of metamaterial layers. Consequently, achieving the required material properties is extremely difficult.

The use of two-dimensional coordinate transformations as quasiconformal mappings has been proposed [4,21], because those result in media with reduced anisotropy and remove the magnetic requirement. Quasiconformal mappings present small deviations in the Cauchy–Riemman equations. An important property of the conformal transformation is the angle preservation among oriented curves in the coordinate system. Proposals of three-dimensional quasiconformal mappings for TO can also be found in [15,22,23].

In particular, in addition to anisotropic properties, the perfect free-space cloak designed by TO also leads to a singularity in the medium. As verified in [3], a point is mapped onto a circle via the coordinate transformation in the conventional perfect cloak, which is the source of this singularity. An alternative approach to invisibility, known as a "carpet cloak," was proposed in [4], where a reflective sheet is deformed without changing the reflected waves, thus creating a hidden area under this deformed reflective sheet. In [4], the authors achieve a quasiconformal coordinate transformation via a grid optimization method with slipping boundary conditions, which leads to almost isotropic material. A practical implementation of this carpet cloak can be found in [24], where the medium is formed by spatially varying the density of 50 nm diameter silicon posts embedded in silicon dioxide.

Although the original proposal for the carpet cloak used quasiconformal mapping [4], other approaches have been investigated [25,26]. In [25], the use of periodically layered graphene is studied to achieve the material requirements for a quasiconformal triangular coordinate transformation that implements the carpet cloak. Also using this coordinate transformation, [26] suggests the manufacturing of a carpet cloak with homogeneous anisotropic material that works for transverse magnetic waves and is made of Al_2O_3 slabs with a Teflon background.

As previously mentioned, the downside to the quasiconformal mapping proposed in [4] is the use of slipping boundary conditions, which lead to reflections at the device boundaries due to discontinuity of the transformation [11]. In addition, this work presents a low ratio between the invisible region and cloak dimensions. An alternative carpet cloak design, with a large invisible region, high cloak ratio, and homogeneous anisotropic media, was presented in [26,27].

In this paper, we propose a strategy to reduce anisotropy in the carpet cloak design. It is based on the parameterization of the coordinate transformation and the use of the least squares method (LSM) presented in [10] to reduce the anisotropy in the carpet cloak without resulting in edge discontinuities. We define the initial (nonconformal) coordinate transformation and the helper function $b(x, y)$ that guarantees boundary continuities and later use the LSM on a variable-degree polynomial series to reduce the original anisotropy. Questions about anisotropy minimization are discussed, such as refractive index contrast and the resulting coordinate transformation usability. Finally, the obtained medias are simulated using the finite element method.

2. CARPET CLOAK TRANSFORMATION

The coordinate transformation functions for the carpet cloak are presented in this section. We also detail the choice of the helper function $b(x, y)$, which limits the effects of the polynomial series at the boundaries to avoid changes in their continuity. This function ensures that the cloaked area does not shrink during the application of the LSM as well.

The coordinate transformation is defined as

$$x' = x + b(x, y)\sum_{i=0}^{p}\sum_{j=0}^{q} A_{ij}x^i y^j$$

$$y' = y + c\left(1 - \frac{y}{h}\right)\cos\left(\frac{\pi x}{w}\right) + b(x, y)\sum_{i=0}^{p}\sum_{j=0}^{q} B_{ij}x^i y^j, \quad (1)$$

where $(x, y) \in [-\frac{w}{2}, \frac{w}{2}] \times [0, h]$ and p and q are the polynomial orders for the series in the x and y coordinates, respectively. Parameters A_{ij} and B_{ij} are zero for the initial transformation, i.e., without anisotropy reduction. This initial transformation is illustrated in Fig. 1.

The transformation Eq. (1) maps the point (0,0) to $(0, c)$, as demonstrated in Fig. 1, defining the region underneath the cloak, which is effectively invisible to an outside observer. This boundary condition provides the cloaking functionality. Furthermore, the transformation continuity is guaranteed at the outer edges of the geometry, at $x = \pm\frac{w}{2}$ and $y = h$. This continuity defines the reflectionless property of our design. We note that the boundary $y = 0$ is perfectly reflective by design [4]. The helper function $b(x, y)$ is defined as

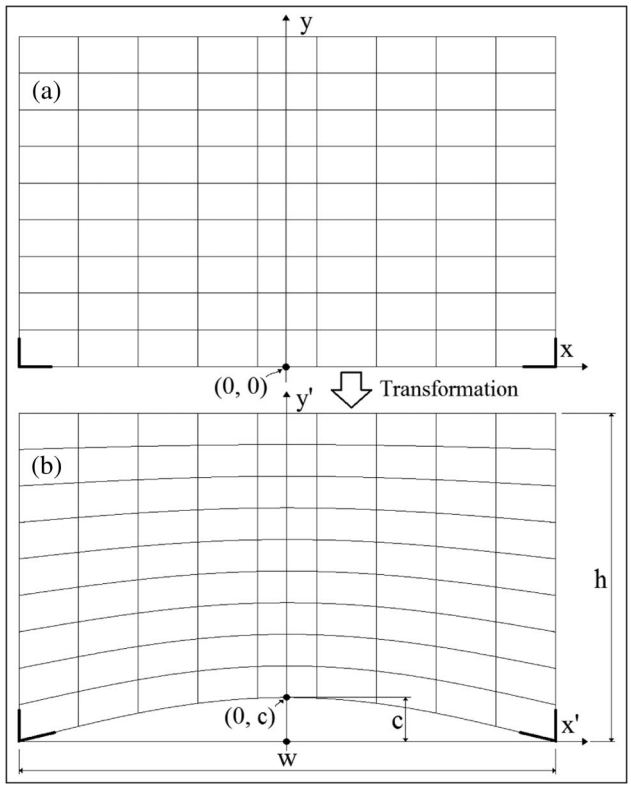

Fig. 1. Initial transformation. (a) Original media. (b) Transformed media.

$$b(x, y) = (x^2 + y)(h - y)\cos\left(\frac{\pi x}{w}\right). \quad (2)$$

This definition guarantees that the parameterization function does not change the boundary conditions around the medium at (0,0), since it vanishes only at that point in the carpet domain due to the term $(x^2 + y)$. Furthermore, it is a continuous function that also vanishes at the outer borders, as required to guarantee the transformation continuity. This choice for the $b(x, y)$ function does not guarantee the shape of the cloaked region. However, it is possible to define the $b(x, y)$ function in order to increment the number of fixed points using, for example,

$$b(x, y) = (h - y)\cos\left(\frac{\pi x}{w}\right)\prod_{n=1}^{N}[(x - x_n)^2 + y]. \quad (3)$$

In Eq. (3), the points $(x_1, 0)\ldots(x_N, 0)$ are fixed and mapped solely by the initial transformation. An increase in the number of fixed points represents more optimization restrictions and greater difficulty in achieving acceptable anisotropy values. Additionally, the resulting transformation becomes less predictable between the fixed points. In the limit where the whole boundary shape is preserved, we could define $b(x, y)$ as

$$b(x,y) = \sin\left(\frac{\pi y}{h}\right)\cos\left(\frac{\pi x}{w}\right). \quad (4)$$

In this case the minimal anisotropy value will be clamped by the lower corners of the transformed region, as illustrated by the thick segments in Fig. 1, because this point has been fixed by the nonconformal boundary condition. At the lower corners of the transformed domain the curves $x' = w/2$ (or $x' = -w/2$) and $y' = 0$ do not intercept at 90° and the coefficients A and B will have no effect there since they are multiplied by zero; as a result, no optimization can be performed there.

If one desires to fix the whole domain boundary, the initial transformation must satisfy the Cauchy–Riemann conditions at least at those lower corner points. An example of initial transformation for the carpet cloak that satisfies those conditions at the lower corners is

$$x' = xy' = y + c\left(1 - \frac{y}{h}\right)\cos\left(\frac{\pi x}{w}\right)^2. \quad (5)$$

Nonetheless, satisfying those conditions is necessary but not sufficient to guarantee anisotropy reduction due to the uniqueness in the Riemann mapping theorem [28]. Indeed, our numerical results confirm that anisotropy cannot be reduced when the transformation in Eq. (5) is used with the definition in Eq. (4), although this initial transformation satisfies the Cauchy–Riemann equations at the lower corners. This a consequence of the $b(x, y)$ function choice. It not only defines the closed region shape but also the coordinate transformation at boundary points that prevent one from finding the Riemann map (that is unique).

It is important to note that the boundary transformation was not fixed in [4] as a result of the *sliding* boundary conditions. That approach allowed anisotropy minimization down to negligible values, tending toward the Riemann map. The downside then is that the boundary media will be inhomogeneous and reflections at those boundaries are unavoidable.

From this discussion, we see that the method in [10] is not able to achieve the conformal map between a closed region to the open unit disk (the Riemann map), because it defines both the boundary shape and the coordinate transformation at the boundary. On the other hand, if the boundary conditions are relaxed to not define a closed region, then arbitrarily small values of anisotropy can be achieved, as is the case when using the definition in Eq. (2).

Finally, the Riemann mapping theorem allows one to conclude that for TO applications, the boundary shapes of which define a closed region, anisotropy cannot be reduced if the transformation is also defined at the whole boundary. Therefore, any method will fail in anisotropy reduction to arbitrarily low values if both conditions are simultaneously met. The above analysis for a carpet cloak exemplifies this concept.

In the next section, we describe the anisotropy minimization results via LSM for different degrees of freedom (DoF) (different values of p and q) using the initial transformation in Eq. (1) and the $b(x, y)$ defined in Eq. (2), where the boundary are not completely defined. Finally, we illustrate the simulated electromagnetic fields distribution of the carpet cloak designs.

3. NUMERICAL RESULTS

In order to perform a numerical test with the anisotropy reduction, we choose $c = 0.2$ μm, $h = 1.5$ μm, and $w = 4$ μm to design the carpet cloak in the general form of the coordinate transformations of Eq. (1). Next, the LSM is used to minimize the anisotropy in the transformation through the $2(p + 1)(q + 1)$ DoF provided by the parameters A_{ij} and B_{ij}.

Table 1 presents, for different values of p and q, the results for the final anisotropy, K, defined as [29]

$$K = \mathrm{tr}\left(\frac{J^T J}{2|J|}\right), \quad (6)$$

where J is the Jacobian of the transformation. The results indicate that anisotropy can be reduced when the number of DoF is increased, according to the results from [10,30]. However, comparing the lowest values for anisotropy achieved in Table 1 with those in [10,30], there seems to be a greater difficulty in reducing the anisotropy for the carpet cloak. This difficulty can be explained by the greater number of boundary conditions that must be satisfied in the carpet cloak: the complete segment on three of the four domain interfaces and a single point at the fourth one, in contrast with two opposite boundaries for the waveguide designs in [10,30]. The required refractive index contrast also increased with the anisotropy reduction, agreeing with previous results in [4,10,11,30].

The freedom provided by the parameterization function, which is limited by the helper function $b(x, y)$, may lead to solutions that cannot be implemented, such as a nonbijective transformation, i.e., a transformation that folds over itself. Additionally, the results might not be appropriate when the transformed medium extends over the $y' < 0$ region depending on the physical conditions, as exemplified by Fig. 2. In practice, this situation could be interpreted as the device being partially buried in the ground. It is not possible to model a constraint preventing this situation through an algebraic approach; however, one possible alternative is to include a restriction such as the inequality $y' \geq 0$ and use a numerical optimization method [11] instead of algebraic optimization [10,30].

The anisotropy reduction effects in the refractive index and in the coordinate transformation geometry can be visualized in Fig. 3, which shows the approximated isotropic refractive index of the original medium, of the resulting medium with

Table 1. Anisotropy Reduction for Varying DoF

p	q	DoF	max(K – 1)	avg(K – 1)	n_{max}	n_{min}
—	—	0	0.074478	0.043923	1.628	1.422
0	0	2	0.030478	0.010206	1.633	1.419
1	1	8	0.013484	0.004251	1.643	1.367
2	2	18	0.012209	0.003663	1.648	1.358
3	3	32	0.008713	0.002912	1.650	1.347
4	4	50	0.008021	0.002893	1.658	1.342
5	5	72	0.007114	0.002405	1.660	1.339
6	6	98	0.006332	0.002173	1.677	1.335
7	7	128	0.005305	0.001801	1.750	1.307
8	8	162	0.004289	0.001457	1.983	1.213
9	9	200	0.003047	0.001082	2.588	1.000

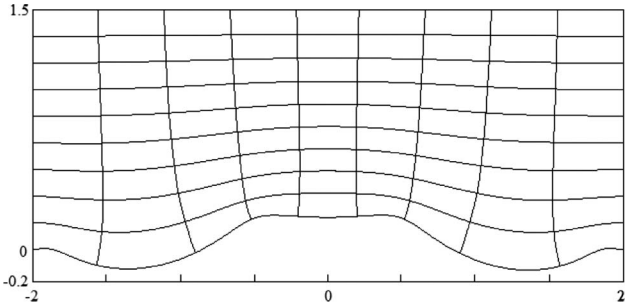

Fig. 2. Anisotropy reduction, with $p = q = 9$, results in undesirable transformation due to the medium extending over the $y' < 0$ region.

$p = q = 6$, and of the resulting medium with $p = q = 9$. The angles in the transformed coordinates in Figs. 3(b) and 3(c) are preserved: All the constant coordinate curves intersect at approximately 90°, in contrast to Fig. 3(a), which has no anisotropy minimization.

Although less effective than in waveguides, good optimization results were obtained for the media using the LSM algorithm without incurring nonbijective transformations or points with $y' < 0$ for $p = q = 6$. A full-wave numerical simulation of the resulting medium was performed for this case to verify the possibility of discarding the residual anisotropy from the transformation. A background medium with refractive index 1.5 is assumed so that regions with index $n < 1$ are not required. The results from Table 1 already include this background medium. As demonstrated in that table, the refractive index range can be achieved by common materials at 750 nm wavelength.

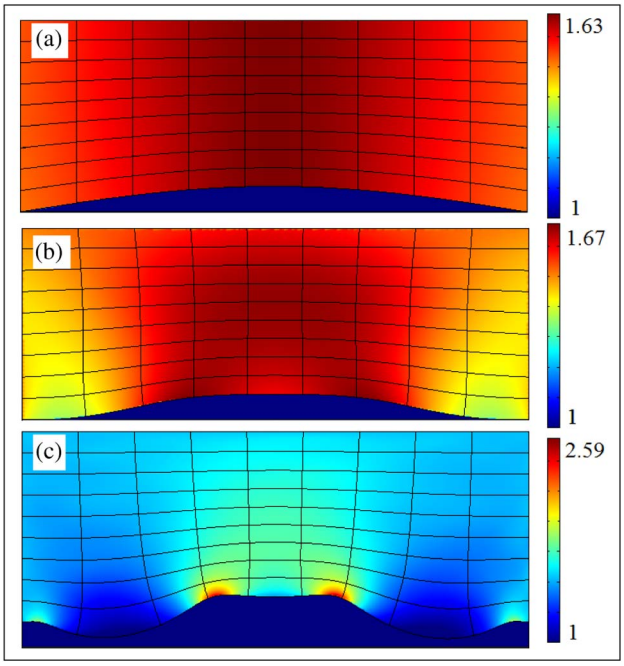

Fig. 3. Refractive index map for (a) original medium, (b) transformed medium with $p = q = 6$, and (c) transformed medium with $p = q = 9$.

Figure 4 presents the results of the simulation where a Gaussian beam with a wavelength of 750 nm reflects at the lower boundary of the device at $y = 0$ for four situations: (a) the original medium where no hidden area exists; (b) the

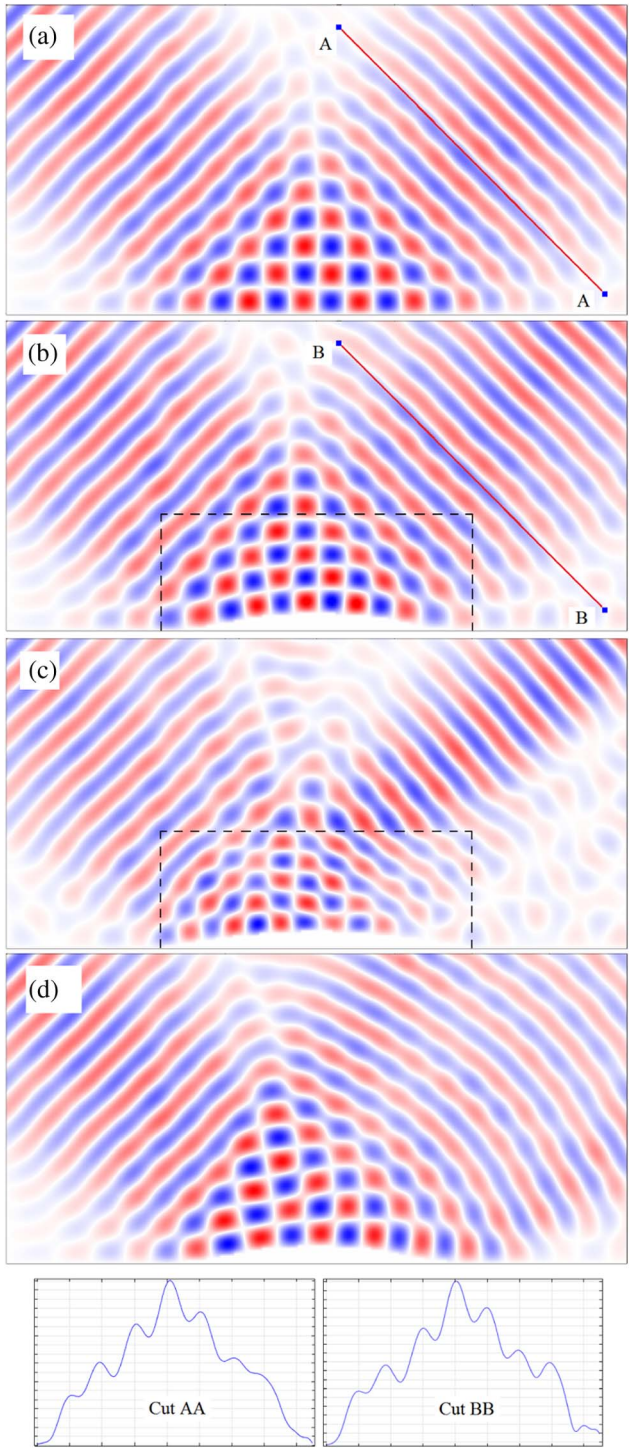

Fig. 4. Normalized electric field plot for a Gaussian beam incident at a 45° angle from the upper left corner and reflecting at the carpet cloak lower boundary. (a) Original media. (b) Isotropic approximation of the carpet cloak for the case $p = q = 6$. (c) Isotropic approximation, without anisotropy reduction. (d) Deformed mirror without a cloak with $p = q = 6$.

transformed medium, with anisotropy minimization using $p = q = 6$, represented under the dashed line, with the cloaked region below the deformation; (c) the transformed medium, without anisotropy reduction; and (d) the deformed mirror without a cloaking device. Those simulation results let us conclude that the anisotropy minimization obtained by the LSM is sufficient to enable the construction of the cloaking device with isotropic materials only. Comparing Figs. 4(a) (CutAA) and 4(b) (CutBB), the electric field patterns outside the carpet cloak are almost indistinguishable. The case in Fig. 4(c) confirms the requirement of anisotropy reduction in the carpet cloak, showing that the reflection distortion is quite visible compared to Fig. 4(a). In the same way, Fig. 4(d) confirms the necessity of a carpet cloak over the deformed reflecting plane. When compared to the original medium, the waveform is not flat at the output, and it is possible to see both phase and amplitude distribution changing in the reflected beam, for instance, in the opposite phase at the upper right corner. With these changes in the reflected beam, the distorted mirror can be readily detected by an observer at output, implying in invisibility loss.

The transformation presented in Fig. 2, with $p = q = 9$, was also simulated. Figure 5(a) shows the electric field for this medium. Figure 5(b) shows the electric field for the deformed mirror without a cloaking device. These results confirm that the mirror geometry is more complicated for $p = q = 9$ than for

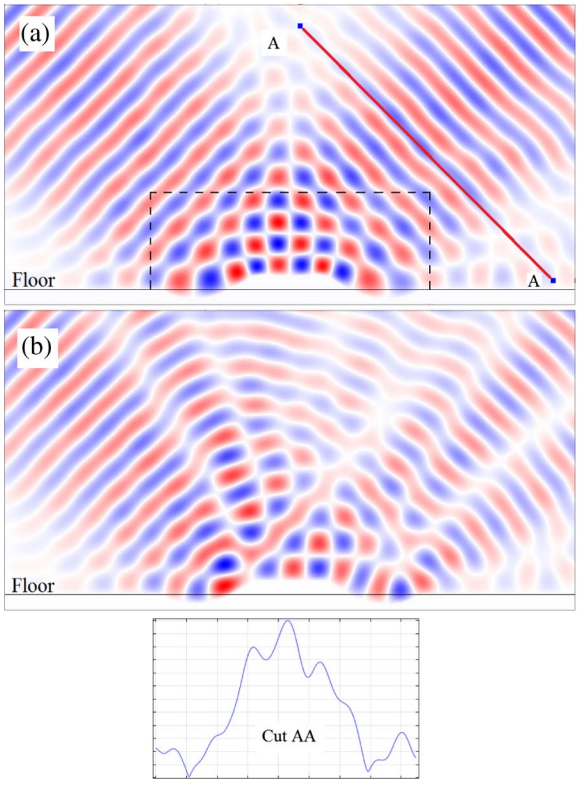

Fig. 5. Normalized electric field plot for a Gaussian beam incident at a 45° angle from the upper left corner and reflecting at the carpet cloak lower boundary. (a) Isotropic approximation of the carpet cloak for the case $p = q = 9$. (b) Deformed mirror without a cloak with $p = q = 9$.

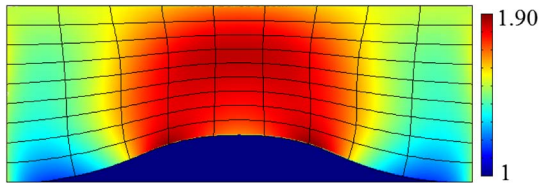

Fig. 6. Refractive index map using $c = 0.4$ μm and $p = q = 4$.

$p = q = 6$. Moreover, comparing the results in Fig. 4(d) with those in Fig. 5(b), the presence of a larger number of beams after reflection in the latter case is notable. The anisotropy reduction mostly compensates for the extra mirror deformations, but not as well as in the case $p = q = 6$ (as can be observed by the electric field norm profile in the cuts). Figure 5 also shows the presence of the electric field within the region $y' < 0$.

The effect of increasing parameter c is also investigated. For the case $c = 0.4$ μm, the initial transformation maximal anisotropy increases from 0.074 ($c = 0.2$ μm) to 0.185. Anisotropy minimization is also more difficult: For example, the case $p = q = 9$ results in a maximal anisotropy of 0.008, more than twice what was obtained previously. Only the resulting index map for the case $p = q = 4$ (maximum anisotropy 0.032) is shown in Fig. 6, once additional increases in p and q lead to points with $n < 1$ and complicated mirror shapes. For the same reasons, only the simulation results for the case $p = q = 4$ are presented in Fig. 7.

As expected, Fig. 7 demonstrates that a carpet cloak with $c = 0.4$ μm has a lower performance than the previous case due to the higher residual anisotropy. Nevertheless, it is still clear that the presence of the cloaking medium greatly improves the distortions in the reflected wave when compared to the uncloaked mirror. Apart from increasing the degrees of the

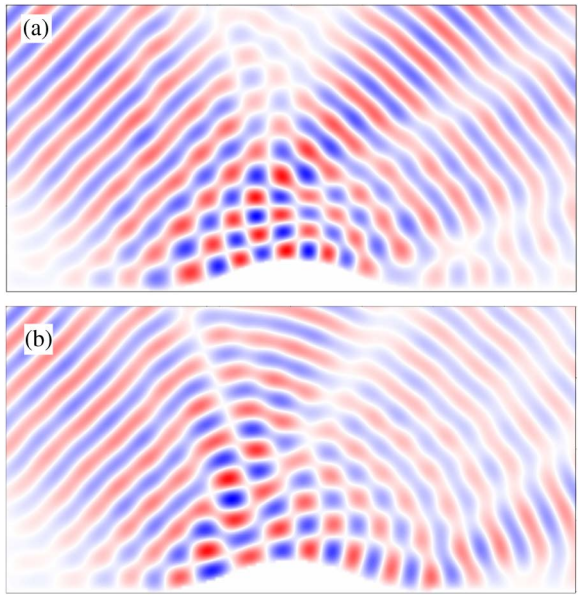

Fig. 7. Normalized electric field plot for a Gaussian beam incident at a 45° angle from the upper left corner and reflecting at the carpet cloak lower boundary ($c = 0.4$ μm). (a) Isotropic approximation of the carpet cloak for the case $p = q = 4$. (b) Deformed mirror without a cloak with $p = q = 4$.

series expansions p and q, an alternative approach to achieving further anisotropy reduction is to allow the interface cloak shape to be arbitrary. That would relax the boundary conditions even further and allow the method to more easily reach the desired Riemann map (although it would probably increase the cloak footprint).

4. CONCLUSION

The design of a reflectionless quasiconformal carpet cloak was presented in this paper through the use of a parameterization strategy optimized via LSM. The details of the initial coordinate transformation and helper function were presented. The effectiveness of the parameterization approach was confirmed by full-wave simulations in example designs. The effects of variations in the DoF were studied showing that this choice might lead to more complex geometries if set too high. We also investigated the effects of the boundary conditions for the transformation in light of the Riemann mapping theorem, presenting deeper insights in the flexibility and limits of TO.

The parameterization strategy has the advantage of guaranteeing transformation continuity with the surrounding media, in contrast to the original carpet cloak. Furthermore, this approach enables the use of restrictions in the refractive index or coordinate transformation and represents an interesting possibility of application for free-space cloaking.

Funding. Conselho Nacional de Desenvolvimento Científico e Tecnológico (CNPq); Coordenação de Aperfeiçoamento de Pessoal de Nível Superior (CAPES); Fundação de Amparo à Pesquisa do Estado de Minas Gerais (FAPEMIG); Universidade Federal de Itajubá (UNIFEI).

REFERENCES

1. U. Leonhardt and T. Philbin, *Geometry and Light: The Science of Invisibility* (Dover, 2010).
2. N. Kundtz, D. Smith, and J. Pendry, "Electromagnetic design with transformation optics," Proc. IEEE **99**, 1622–1633 (2011).
3. J. B. Pendry, D. Schurig, and D. R. Smith, "Controlling electromagnetic fields," Science **312**, 1780–1782 (2006).
4. J. Li and J. B. Pendry, "Hiding under the carpet: a new strategy for cloaking," Phys. Rev. Lett. **101**, 203901 (2008).
5. W. Cai, U. K. Chettiar, A. V. Kildishev, V. M. Shalaev, and G. W. Milton, "Nonmagnetic cloak with minimized scattering," Appl. Phys. Lett. **91**, 111105 (2007).
6. H. F. Ma, W. X. Jiang, X. M. Yang, X. Y. Zhou, and T. J. Cui, "Compact-sized and broadband carpet cloak and free-space cloak," Opt. Express **17**, 19947–19959 (2009).
7. J. Zhang, Y. Luo, H. Chen, and B.-I. Wu, "Cloak of arbitrary shape," J. Opt. Soc. Am. B **25**, 1776–1779 (2008).
8. U. Leonhardt, "Perfect imaging without negative refraction," New J. Phys. **11**, 093040 (2009).
9. J. Hunt, G. Jang, and D. R. Smith, "Perfect relay lens at microwave frequencies based on flattening a Maxwell lens," J. Opt. Soc. Am. B **28**, 2025–2029 (2011).
10. M. A. F. C. Junqueira, L. H. Gabrielli, and D. H. Spadoti, "Anisotropy minimization via least squares method for transformation optics," Opt. Express **22**, 18490–18498 (2014).
11. D. Liu, L. H. Gabrielli, M. Lipson, and S. G. Johnson, "Transformation inverse design," Opt. Express **21**, 14223–14243 (2013).
12. Z. Chang, X. Zhou, J. Hu, and G. Hu, "Design method for quasi-isotropic transformation materials based on inverse Laplace's equation with sliding boundaries," Opt. Express **18**, 6089–6096 (2010).
13. Y. G. Ma, N. Wang, and C. K. Ong, "Application of inverse, strict conformal transformation to design waveguide devices," J. Opt. Soc. Am. A **27**, 968–972 (2010).
14. C. García-Meca, M. M. Tung, J. V. Galán, R. Ortuño, F. J. Rodríguez-Fortuño, J. Martí, and A. Martínez, "Squeezing and expanding light without reflections via transformation optics," Opt. Express **19**, 3562–3575 (2011).
15. H. F. Ma and T. J. Cui, "Three-dimensional broadband and broad-angle transformation-optics lens," Nat. Commun. **1**, 124 (2010).
16. D. H. Spadoti, L. H. Gabrielli, C. B. Poitras, and M. Lipson, "Focusing light in a curved-space," Opt. Express **18**, 3181–3186 (2010).
17. J. Zhou, M. Li, L. Xie, and D. Liu, "Design of a new kind of polarization splitter based on transformation optics," Optik **122**, 1672–1675 (2011).
18. D.-H. Kwon and D. H. Werner, "Polarization splitter and polarization rotator designs based on transformation optics," Opt. Express **16**, 18731–18738 (2008).
19. D. Schurig, J. J. Mock, B. J. Justice, S. A. Cummer, J. B. Pendry, A. F. Starr, and D. R. Smith, "Metamaterial electromagnetic cloak at microwave frequencies," Science **314**, 977–980 (2006).
20. H. Chen, C. T. Chan, and P. Sheng, "Transformation optics and metamaterials," Nat. Mater. **9**, 387–396 (2010).
21. L. Ahlfors, *Lectures on Quasiconformal Mappings*, University Lecture Series (American Mathematical Society, 1966).
22. C. García-Meca, R. Ortuño, J. Martí, and A. Martínez, "Full three-dimensional isotropic transformation media," New J. Phys. **16**, 023030 (2014).
23. N. I. Landy, N. Kundtz, and D. R. Smith, "Designing three-dimensional transformation optical media using quasiconformal coordinate transformations," Phys. Rev. Lett. **105**, 193902 (2010).
24. L. H. Gabrielli, J. Cardenas, C. B. Poitras, and M. Lipson, "Silicon nanostructure cloak operating at optical frequencies," Nat. Photonics **3**, 461–463 (2009).
25. R. Zhang, X. Lin, L. Shen, Z. Wang, B. Zheng, S. Lin, and H. Chen, "Free-space carpet cloak using transformation optics and graphene," Opt. Lett. **39**, 6739–6742 (2014).
26. N. Wang, M. Mukhtar, Y. Ma, R. Huang, and C. K. Ong, "Homogeneous anisotropic dielectric invisibility carpet cloak made of Al_2O_3 plates," Europhys. Lett. **104**, 14003 (2013).
27. J. Zhang, L. Liu, Y. Luo, S. Zhang, and N. A. Mortensen, "Homogeneous optical cloak constructed with uniform layered structures," Opt. Express **19**, 8625–8631 (2011).
28. Z. Nehari, *Conformal Mapping*, International Series in Pure and Applied Mathematics (McGraw-Hill, 1952).
29. K. Astala, T. Iwaniec, and G. Martin, *Elliptic Partial Differential Equations and Quasiconformal Mappings in the Plane (PMS-48)*, Princeton Mathematical Series (Princeton University, 2008).
30. M. Junqueira, L. Gabrielli, and D. Spadoti, "Comparison of anisotropy reduction strategies for transformation optics designs," IEEE Photon. J. **7**, 1–10 (2015).